Dependence of Protein Stability on the Structure of the Denatured State: Free Energy Calculations of I56V Mutation in Human Lysozyme

Yuji Sugita and Akio Kitao
Department of Chemistry, Graduate School of Science, Kyoto University, Kyoto 606-8502, Japan

ABSTRACT Free energy calculations were carried out to understand the effect of the I56V mutation of human lysozyme on its thermal stability. In the simulation of the denatured state, a short peptide including the mutation site in the middle is employed. To study the dependence of the stability on the denatured-state structure, five different initial conformations, native-like, extended, and three random-coil-like conformations, were examined. We found that the calculated free energy difference, $\Delta\Delta G^{cal}$, depends significantly on the structure of the denatured state. When native-like structure is employed, $\Delta\Delta G^{cal}$ is in good agreement with the experimental free energy difference, $\Delta\Delta G^{exp}$, whereas in the other four models, $\Delta\Delta G^{cal}$ differs sharply from $\Delta\Delta G^{exp}$. It is therefore strongly suggested that the structure around the mutation site takes a native-like conformation rather than an extended or random-coil conformation. From the free energy component analysis, it has been shown that free energy components originating from Lennard-Jones and covalent interactions dominantly determine $\Delta\Delta G^{cal}$. The contribution of protein-protein interactions to the nonbonded component of $\Delta\Delta G^{cal}$ is about the same as that from protein-water interactions. The residues that are located in a hydrophobic core (F3, L8, Y38, N39, T40, and I89) contribute significantly to the nonbonded free energy component of $\Delta\Delta G^{cal}$. We also propose a general computational strategy for the study of protein stability that is equally conscious of the denatured and native states.

INTRODUCTION

One of the fundamental problems in protein research is how the native protein structures are stabilized by complex physical interactions (Fersht and Serrano, 1993; Mathews, 1993). To understand this problem, mutational analyses have been carried out systematically in proteins such as barnase (Kellis et al., 1989), chymotrypsin inhibitor 2 (CI2) (Otzen and Fersht, 1995; Otzen et al., 1995), staphylococcal nuclease (Shortle et al., 1990), T4 lysozyme (Eriksson et al., 1992), and human lysozyme (Takano et al., 1995, 1997; Funahashi et al., 1996). In most cases, the thermodynamic changes caused by mutations, i.e., the free energy difference, $\Delta\Delta G$, have been explained only in terms of the structural changes in the native state. This is due to the fact that structures of the denatured states are not well characterized experimentally. However, it should be noted that $\Delta\Delta G$ is defined as the difference between the free energy shift caused by mutation in the native state, ΔG_N, and that in the denatured state, ΔG_D. The explanation based only on the structure of the native state is valid only when the stability of the denatured state does not change for the mutation. In this paper we calculate $\Delta\Delta G$ by computer simulations and explain the results in terms of the denatured as well as the native state structures.

Free energy calculation based on molecular dynamics (MD) simulation has now become a common tool for protein research (Beveridge and DiCapua, 1989; Straatsma and McCammon, 1992; van Gunsteren and Mark, 1992; Kollman, 1993). In its applications to the studies of protein stability, free energy calculations are performed for both the native and denatured states. In the native state simulation, a structure determined by x-ray crystallography is employed as an initial structure. On the other hand, a model structure is used in the denatured state simulation, because there is no structure experimentally determined in atomic detail.

In the preceding studies, a short peptide including the mutation site in the middle has been employed in the denatured state simulation (Tidor and Karplus, 1991; Yun-yu et al., 1993; Saito and Taminura, 1995; Sun et al., 1996; Tanimura and Saito, 1996). This treatment involves the approximation that only the neighboring residues of the mutation site contribute significantly to the free energy change in the denatured state. In our previous paper, the validity of the approximation was discussed in the case of CI2 (Sugita and Kitao, 1998). As a starting structure in the free energy calculation, the extended conformation has frequently been employed for the peptide (extended model) by assuming that a protein is fully unfolded in the denatured state. This assumption is expected to be valid when the denaturation is caused by strong denaturants such as GdmCl. However, in recent experimental studies, it has been shown that the residual structure exists to some extent even in the denatured state and that the structure becomes more compact as the denaturation conditions become milder (Buck et al., 1994; Dill and Shortle, 1991; Evans et al., 1991; Radford et al., 1992; Flanagan et al., 1993; Kataoka and Goto, 1996; Lattman, 1994; Shortle, 1996). In these cases, it is unlikely that the extended model can be an appropriate model for the denatured state. In this paper, we employ five different conformations, including an extended one, as initial structures of the simulations. By comparing

Received for publication 9 January 1998 and in final form 22 June 1998.
Address reprint requests to Dr. Akio Kitao, Department of Chemistry, Graduate School of Science, Kyoto University, Kitashirakawa Oiwake-chou, Sakyo-ku, Kyoto 606-8502, Japan. Tel.: 81-75-753-3670; Fax: 81-75-753-3669; E-mail: kitao@qchem.kuchem.kyoto-u.ac.jp.

0006-3495/98/11/2178/10 $2.00

the results with the experimental free energy difference, $\Delta\Delta G^{exp}$, we discuss a possible residual structure near the mutation site in the denatured state. This is the first purpose of this study.

The second purpose is to decompose the calculated free energy, $\Delta\Delta G^{cal}$, into several components, such as covalent, Lennard-Jones, and electrostatic terms. Free energy component analysis gives detailed information, which helps us to understand the mechanism of the stability change caused by the mutation. Although the components of the free energy are path-dependent, they have significant meanings when the path is thoughtfully chosen and clearly defined (Smith and van Gunsteren, 1994; Boresch et al., 1994; Boresch and Karplus, 1995; Brady and Sharp, 1995; Brady et al., 1996).

In free energy calculation, there is one difficulty to be solved, i.e., $\Delta\Delta G$ is very small, typically on the order of a few kcal/mol for single mutation. To obtain $\Delta\Delta G^{cal}$ comparable to $\Delta\Delta G^{exp}$ in accuracy, it is essential to establish a simulation methodology by carefully examining simulation algorithms (Yun-yu et al., 1993; Saito and Taminura, 1995). In our calculation, we used a newly developed program for free energy calculation by more accurate treatments of nonbonded interactions. The performance of the developed software package has been demonstrated elsewhere for the case of V57A mutation of CI2 (Sugita and Kitao, 1998).

In this paper, we study a single-site mutation of human lysozyme. Recently, systematic mutation analyses have been carried out for this molecule (Takano et al., 1995, 1997; Funahashi et al., 1996). Thermodynamic changes as well as structural changes in the native states caused by the substitutions of I by V have been reported (Takano et al., 1995). In the case of hen egg lysozyme, it has been shown that hydrophobic clusters persist in a thermally denatured state (Evans et al., 1991). Judging from these preceding works, the extended model may not be appropriate in the case of human lysozyme.

Among five I-to-V mutations that have been studied experimentally, we have chosen the I56V mutation for the present study for the following two reasons: 1) The mutation site, I56, is located in the middle of a β-turn structure in the native state (Fig. 1). It is of interest to investigate whether the native-like structure around the mutation site is preserved even in the denatured state, in which only local interactions should be operative. 2) $\Delta\Delta G$ of the I56V mutation has been the largest of the five substitutions of I by V, whereas the structural changes in the native state were the smallest (Takano et al., 1995). This suggests that a large free energy change is taking place in the denatured state. By using free energy component analysis for different denatured state models, we try to understand the physical nature of I56V mutation.

METHOD

In this section, we briefly describe the methods of free energy calculation to clearly define the notations in this paper, although the theory of free energy calculation is well established in the references (Beveridge and DiCapua, 1989; Straatsma and McCammon, 1992; van Gunsteren and Mark, 1992; Kollman, 1993). The Gibbs free energy changes between wild-type and mutant proteins are defined as (Tidor and Karplus, 1991; Yun-yu et al., 1993; Saito and Taminura, 1995; Sun et al., 1996; Tanimura and Saito, 1996)

$$\begin{array}{ccc} & \overset{\Delta G_W}{\rightarrow} & \\ W_N & & W_D \\ {\scriptstyle \Delta G_N}\downarrow & & \downarrow{\scriptstyle \Delta G_D} \\ M_N & \underset{\Delta G_M}{\rightarrow} & M_D \end{array}, \qquad (1)$$

where W_N, W_D, M_N, and M_D represent wild-type protein in the native state, wild-type in the denatured state, mutant in the native state, and mutant in the denatured state, respectively. The denaturation free energy changes, ΔG_W and ΔG_M, are determined by experimental methods, such as calorimetry, whereas the mutation free energy changes in the native state, ΔG_N, and in the denatured state, ΔG_D, are obtained by theoretical methods, such as free energy perturbation (FEP) or thermodynamic integration (TI). A comparison between the calculated and experimental values is made by using the relation $\Delta\Delta G = \Delta G_W - \Delta G_M = \Delta G_N - \Delta G_D$. It should be noted that the simulations of both the native and denatured states are required to calculate $\Delta\Delta G$.

First, a Hamiltonian $H(\lambda)$ is introduced. The coupling parameter, λ, takes a value between zero and unity, corresponding to the path from W_N to M_N or from W_D to M_D. In other words, $H(\lambda)$ is defined to satisfy the conditions $H(0) = H_W$ and $H(1) = H_M$, where H_W and H_M are the Hamiltonians of the wild-type and mutant, respectively. In FEP, the Gibbs free energy change from wild-type to mutant, ΔG, which is either ΔG_N or ΔG_D, is given by

$$\Delta G = -k_B T \sum_i \ln\langle \exp[-\Delta H(\lambda_i)/k_B T]\rangle_{\lambda_i}, \qquad (2)$$

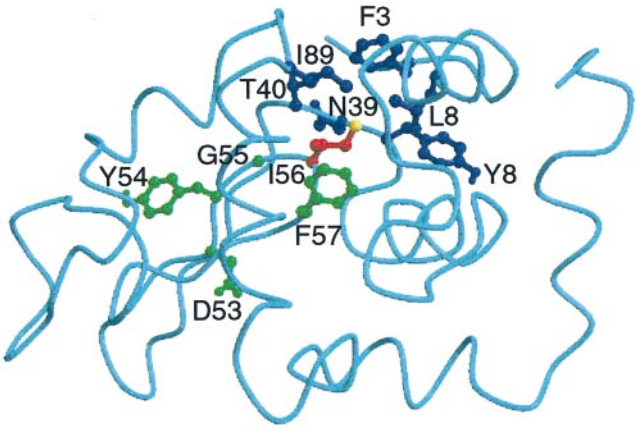

FIGURE 1 The native state structure of human lysozyme. Heavy atoms of the mutated residue I56 (*red*); the mutated methyl group (*yellow*); the residues F3, L8, Y38, N39, T40, and I89 (*blue*); and the residues D53, Y54, G55, and F57 (*green*). This figure was created with Molscript (Kraulis, 1991) and Raster3d (Merrit and Murphy, 1994).

where $\langle \cdots \rangle_{\lambda_i}$ represents the isothermal-isobaric ensemble average obtained by using hamiltonian $H(\lambda_i)$ and $\Delta H(\lambda_i) = H(\lambda_{i+1}) - H(\lambda_i)$. In TI, ΔG is given by

$$\Delta G = \int_0^1 \left\langle \frac{\partial H(\lambda)}{\partial \lambda} \right\rangle_\lambda d\lambda. \tag{3}$$

In TI, ΔG can be decomposed into free energy components. The free energy change is divided into covalent (ΔG_{cov}), Lennard-Jones (ΔG_{LJ}), electrostatic (ΔG_{el}), and reaction field (ΔG_{RF}) components,

$$\begin{aligned} \Delta G &= \Delta G_{cov} + \Delta G_{LJ} + \Delta G_{el} + \Delta G_{RF} \\ &= \Delta G_{cov} + \Delta G_{nonbd} + \Delta G_{RF}, \end{aligned} \tag{4}$$

where the nonbonded component, ΔG_{nonbd}, is defined as the sum of ΔG_{LJ} and ΔG_{el}. It has been shown that ΔG_{RF}, which originates from the reaction field energy (Beglov and Roux, 1994), is negligible when the net charge of the system does not change for the mutation (Sugita and Kitao, 1998). Because net charge is constant and ΔG_{RF} is negligible in the present study, we do not mention ΔG_{RF} in the following sections. ΔG_{nonbd} can also be divided into the atomic free energy changes, $\Delta G_{atom\ i}$, and the residual free energy changes, $\Delta G_{residue\ \alpha}$, as follows:

$$\begin{aligned} \Delta G_{nonbd} &= \sum_i \Delta G_{atom\ i} \\ &= \sum_i \left[\frac{1}{2} \sum_j \Delta G_{atom\ pair\ ij} \right] \end{aligned} \tag{5}$$

$$\begin{aligned} \Delta G_{nonbd} &= \sum_\alpha \Delta G_{residue\ \alpha} \\ &= \sum_\alpha \left[\sum_{\substack{atoms \\ in\ residue\ \alpha}} \Delta G_{atom\ i} \right], \end{aligned} \tag{6}$$

where $\Delta G_{atom\ pair\ ij}$ is a free energy component originating from the nonbonded interaction between atoms *i* and *j*.

As mentioned in the Introduction, free energy components are intrinsically path-dependent. A path employed in the calculation must be defined clearly, otherwise free energy components are meaningless (Smith and van Gunsteren, 1994; Boresch et al., 1994; Boresch and Karplus, 1995; Brady and Sharp, 1995; Brady et al., 1996). The path is determined by the way in which the coupling parameter λ is changed. In this study, the single coupling parameter is used for all energy terms, as already shown in Eqs. 2 and 3.

In the denatured state simulation, a five-residue peptide including the mutation site in the middle (peptide model) is employed (Tidor and Karplus, 1991; Yun-yu et al., 1993; Saito and Taminura, 1995; Sun et al., 1996; Tanimura and Saito, 1996). Here we clarify assumptions involved with the peptide model used in the calculation of ΔG_D. First the system is classified into three parts: residues included in the peptide model (pept), the rest of the residues (rest), and water molecules (wat). Considering the interactions among these three parts, the free energy change can be decomposed into three terms,

$$\Delta G = \Delta G_{pept\text{-}pept} + \Delta G_{pept\text{-}wat} + \Delta G_{pept\text{-}rest}, \tag{7}$$

where $\Delta G_{pept\text{-}pept}$, $\Delta G_{pept\text{-}wat}$, and $\Delta G_{pept\text{-}rest}$ are free energy changes caused by the interactions among the peptide part, between the peptide and water molecules, and between the peptide and the rest. In the native-state simulation, all terms are considered in the calculation. In the peptide model for the denatured state, the last term in Eq. 7, $\Delta G_{pept\text{-}rest}$, is assumed to be negligible. The nonbonded component, ΔG_{nonbd}, can be partitioned into the components originating from protein-protein interactions ($\Delta G_{pro\text{-}pro}$) and from protein-water interactions ($\Delta G_{pro\text{-}wat}$). $\Delta G_{pro\text{-}pro}$ in the native state is a sum of nonbonded parts in $\Delta G_{pept\text{-}pept}$ and $\Delta G_{pept\text{-}rest}$, whereas in the peptide model of the denatured state, $\Delta G_{pro\text{-}pro}$ is identical to the nonbonded part in $\Delta G_{pept\text{-}pept}$.

To examine the structural dependence on $\Delta G_{pept\text{-}pept}$ and $\Delta G_{pept\text{-}wat}$, five different initial structures were prepared. In the first model, which is termed the "native-like" model, the initial coordinates of the peptide were taken from the x-ray structure of the corresponding region. To sample conformational space in the vicinity of the initial conformation, we added some constraints for backbone atoms. In the second model, the initial conformation is an extended form, i.e., all of the main-chain dihedral angles are taken to be equal to 180° (the extended model). Because no constraints are added in the extended model, conformation is expected to be more flexible.

The third model involves the random-coil state. In the random-coil state, a protein fluctuates over a large conformational space. Instead of performing a very long simulation to sample a large conformational space, we carried out three simulations starting from the different initial structures. An average of $\Delta\Delta G^{cal}$ obtained from three calculations is regarded as $\Delta\Delta G$ when the structure in the denatured state is assumed to be random coil. Three different structures were generated by the following procedure. MD in vacuum was performed at high temperature (1000 K), starting from the extended structure. Three structures are selected from a MD trajectory every 300 ps. The root mean square deviations (RMSDs) of backbone atoms from the extended and native-like structures are shown in Table 1.

TABLE 1 Peptide models for the denatured state

Denatured state model	RMSD* (Å)	RMSD# (Å)	No. of water molecules
Extended (EXT)	—	4.863	1062
Native-like (NTV)	4.863	—	1063
Random-coil-like 1 (RND1)	3.614	1.728	1064
Random-coil-like 2 (RND2)	1.888	3.407	1059
Random-coil-like 3 (RND3)	2.389	3.353	1060

*RMSDs of backbone atoms from the extended structure.
#RMSDs of backbone atoms from the native-like structure.

The five structures employed in free energy calculations are mutually distant in conformational space.

As listed in Table 1, EXT, NTV, RND1, RND2, and RND3 represent the extended model, the native-like model, and the random-coil-like models 1, 2, and 3 for the denatured state, respectively. We have also created abbreviations for ΔG_D and $\Delta\Delta G^{cal}$. ΔG_D^{NTV}, ΔG_D^{EXT}, ΔG_D^{RND1}, ΔG_D^{RND2}, and ΔG_D^{RND3} represent ΔG_D of the corresponding models of the denatured state. $\Delta\Delta G^{NTV}$, $\Delta\Delta G^{EXT}$, $\Delta\Delta G^{RND1}$, $\Delta\Delta G^{RND2}$, and $\Delta\Delta G^{RND3}$ represent $\Delta\Delta G^{cal}$ when the corresponding models of the denatured state are employed.

Atomic coordinates determined by x-ray crystallography were employed as the initial coordinates of human lysozyme, 196 crystal water molecules, and one sodium ion in the native-state simulation. An additional 4484 water molecules were placed around the protein to fill a sphere of 34-Å radius. A five-residue peptide including the mutation site in the middle, ACE-Y-G-I-F-Q-NME, was used in the denatured state simulations. As discussed above, we prepared five different structures of the peptide. These peptides were solvated by water molecules to fill a sphere of 20 Å. The number of water molecules included in each denatured system is listed in Table 1. In both the native and denatured states, there are roughly three or more layers of water molecules around the solute molecule.

Energy functions and algorithms of the MD simulations are the same as those we have employed previously (Sugita and Kitao, 1998). The AMBER all-atom energy function (Weiner et al., 1986) was used for the protein and peptide molecules, and the TIP3P model (Jorgensen et al., 1983) was employed for water molecules. Spherical Solvent Boundary Potential (SSBP) (Beglov and Roux, 1994) was applied to the system, and Cell Multipole Method (CMM) (Ding et al., 1992) was employed to evaluate nonbonded interactions within the sphere. Each state is simulated in an isothermal-isobaric ensemble. To achieve isothermal conditions at 300 K, the Nosé-Hoover algorithm (Hoover, 1985; Nosé, 1984) is introduced. Isobaric conditions at 1 atm are realized by SSBP. Water molecules are treated as a rigid body. The time step of the MD, Δt, is 0.5 fs.

Except for NTV, all of the systems were equilibrated by the following procedure. 1) An energy minimization of 2000 steps is carried out, with a large value of constraint for restricting protein heavy atoms and crystal water molecules to the initial positions. 2) A 50-ps MD is performed to equilibrate the system to 300 K and 1 atm, by gradually relaxing the constraints. 3) A 50-ps MD is performed without constraints. In NTV, mild constraints for restricting peptide backbone atoms to the native positions are added during the equilibration and the free energy calculation to maintain the structure.

Free energy calculations in both the native and denatured states were carried out in 20 successive stages by changing the coupling parameter λ_i as $\lambda_i = 0.025, 0.075, \ldots, 0.975$ and by using the double wide sampling (Jorgensen and Ravimohan, 1985). At each λ_i, a 5.0-ps MD simulation was performed to equilibrate the system. From the final step of the equilibration, a 5.0-ps MD was continued to calculate ΔG. In total, 200 ps free energy calculations were performed both in the forward (I to V) and the reverse (V to I) directions.

All of the MD/FEP/TI calculations were performed by a newly developed program package (Sugita and Kitao, 1998) based on the framework of the Minimization/MD program PRESTO (Morikami et al., 1992). Subroutines for calculating SSBP were kindly provided by Prof. Benoît Roux.

RESULTS

Free energy differences

Free energy changes, ΔG_N and ΔG_D, determined by FEP and TI are listed in Table 2. The convergence of ΔG is examined by the following two criteria. First, differences

TABLE 2 Free energy differences obtained by FEP and TI treatments

Method	Denatured state model	ΔG_N (kcal/mol)*	ΔG_D (kcal/mol)*	$\Delta\Delta G^{cal}$ (kcal/mol)#	$\lvert\Delta\Delta G^{cal} - \Delta\Delta G^{exp}\rvert$ (kcal/mol)§
FEP	EXT	−0.00 ± 0.20	−2.39 ± 0.06	2.39 ± 0.21	1.20
TI	EXT	−0.02 ± 0.21	−2.40 ± 0.06	2.38 ± 0.22	1.19
FEP	NTV	−0.00 ± 0.20	−1.02 ± 0.13	1.02 ± 0.24	0.18
TI	NTV	−0.02 ± 0.21	−1.01 ± 0.12	0.99 ± 0.24	0.21
FEP	RND1	−0.00 ± 0.20	−1.92 ± 0.49	1.91 ± 0.53	0.72
TI	RND1	−0.02 ± 0.21	−1.90 ± 0.48	1.88 ± 0.53	0.69
FEP	RND2	−0.00 ± 0.20	−2.09 ± 0.14	2.09 ± 0.24	0.90
TI	RND2	−0.02 ± 0.21	−2.10 ± 0.14	2.08 ± 0.25	0.89
FEP	RND3	−0.00 ± 0.20	−2.08 ± 0.98	2.08 ± 1.00	0.89
TI	RND3	−0.02 ± 0.21	−2.12 ± 0.97	2.10 ± 1.00	0.91
FEP	Average¶	−0.00 ± 0.20	−2.03 ± 0.64	2.03 ± 0.64	0.85
TI	Average¶	−0.02 ± 0.21	−2.04 ± 0.64	2.02 ± 0.64	0.84

*Values shown after ± represent the hysteresis errors, defined as $|\Delta G(\text{forward}) - \Delta G(\text{reverse})|/2$, in which ΔG is either ΔG_N or ΔG_D.

#Values shown after ± represent the standard deviation of four values, $\Delta G_N(\text{forward}) - \Delta G_D(\text{forward})$, $\Delta G_N(\text{forward}) - \Delta G_D(\text{reverse})$, $\Delta G_N(\text{reverse}) - \Delta G_D(\text{forward})$, and $\Delta G_N(\text{reverse}) - \Delta G_D(\text{reverse})$.

§The experimental free energy difference ($\Delta\Delta G^{exp}$) is 1.2 ± 0.1 kcal/mol (Takano et al., 1995).

¶"Average" represents the average values over RND1, RND2, and RND3.

between ΔG obtained by FEP and that obtained by TI should be negligibly small if ΔG has been converged. The differences were less than 0.1 kcal/mol in all cases. Second, hysteresis errors (the values after $\pm$) were reasonably small in the case of the native state, NTV, EXT, and RND2. These two results indicate that ΔG_N, ΔG_D^{NTV}, ΔG_D^{EXT}, and ΔG_D^{RND2} have converged well. In the cases of RND1 and RND3, hysteresis errors were larger than in the other cases. These hysteresis errors were caused by the drifts of the peptide structures during the free energy calculations.

As shown in Table 2, ΔG_N was negligibly small compared with ΔG_D. This indicates that $\Delta\Delta G$ is dominantly determined by ΔG_D. In each model of the denatured state, the mutant was energetically more stable than the wild-type protein. Thus, in all cases, $\Delta\Delta G^{cal}$ is always positive. However, the magnitude of $\Delta\Delta G^{cal}$ was significantly dependent on the models of the denatured state. The free energy difference $\Delta\Delta G^{NTV}$, 1.02 $\pm$ 0.24 kcal/mol, was in good agreement with $\Delta\Delta G^{exp}$, 1.2 $\pm$ 0.1 kcal/mol (Takano et al., 1995), whereas $\Delta\Delta G^{EXT}$ was much greater than $\Delta\Delta G^{exp}$. Free energy differences, $\Delta\Delta G^{RND1}$, $\Delta\Delta G^{RND2}$, $\Delta\Delta G^{RND3}$, and their average were also much larger than $\Delta\Delta G^{exp}$. Judging from these results, NTV is the most appropriate model for the denatured state. Free energy differences obtained by NTV and EXT using TI are analyzed further in detail to understand the effect of I56V mutation on protein stability. EXT is chosen as the representative of the unsuitable models of the denatured state in the case of this mutation.

Fluctuation in each model

The RMSD of backbone atoms between these two models after equilibration MD, after forward calculation, and after reverse calculation are 3.46, 3.78, and 3.50 Å, respectively. During the 100-ps equilibration MD and 400-ps free energy calculation, the structure of EXT stayed significantly different from that of NVT. To show dihedral angle fluctuations during the free energy calculations, distributions of (ϕ, ψ) angles of the mutated residue are shown in Fig. 2. For comparison, the distribution in the native state is also shown. The RMSDs of (ϕ, ψ) angles in the native state, EXT, and NTV are (8.1, 7.6), (15.1, 19.0), and (11.0, 11.4), respectively (in degrees). The distribution of dihedral angles in EXT spreads over a larger conformational space than those in NTV and the native state. The fluctuation of NTV is slightly larger than that of the native state. Because the constraints were added to the backbone atoms of NTV, the distribution was determined by the strength of the constraints. Their effect on $\Delta\Delta G^{cal}$ is examined in the Discussion.

Analysis of interactions which dominantly determine free energy difference

In Fig. 3, the free energy change (ΔG), covalent (ΔG_{cov}), Lennard-Jones (ΔG_{LJ}), and electrostatic (ΔG_{el}) components

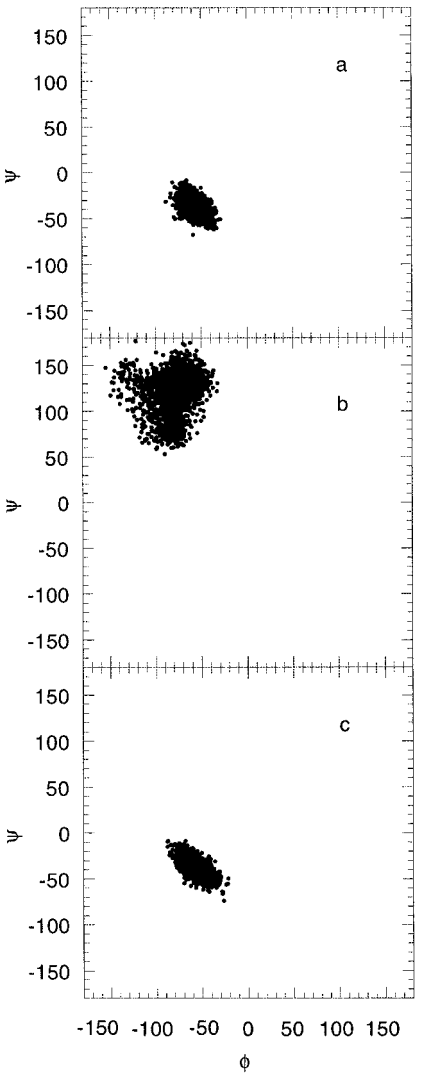

FIGURE 2 The distribution of angles ϕ, ψ of the mutated residue (*a*) in the native state, (*b*) EXT, and (*c*) NTV, respectively, during the free energy calculations.

at each λ are shown. Each component obtained by forward and reverse calculations agreed well at each λ. An excellent reversibility of free energy difference, as well as free energy components, is reflected in the small hysteresis error given in Table 2.

In Table 3, covalent (ΔG_{cov}), Lennard-Jones (ΔG_{LJ}), and electrostatic (ΔG_{el}) components are listed. Covalent and electrostatic components of ΔG_N, ΔG_D^{NTV}, and ΔG_D^{EXT} are positive, whereas Lennard-Jones components are negative. In the native state, positive covalent and electrostatic components cancel the negative Lennard-Jones component. The difference between ΔG_D^{NTV} and ΔG_D^{EXT} originated mainly from the difference in nonbonded contributions, i.e., ΔG_{LJ} and ΔG_{el}. Because ΔG_N is negligibly small, the difference between $\Delta\Delta G^{NTV}$ and $\Delta\Delta G^{EXT}$ originated mainly from the difference in ΔG_{nonbd} in the denatured state. In $\Delta\Delta G^{NTV}$, the contribution of $\Delta\Delta G_{el}$ is negligibly small. The other two

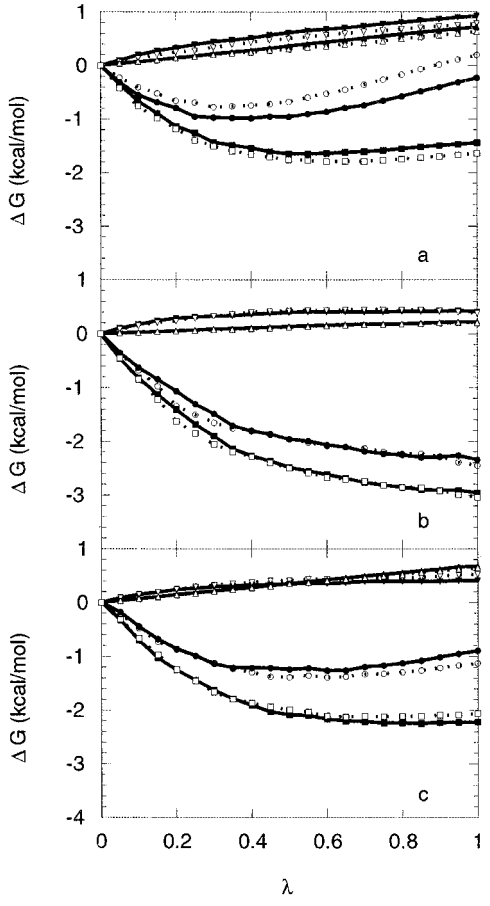

FIGURE 3 λ dependence of the free energy change (●, ○), the covalent term (▼, ▽), the Lennard-Jones term (■, □), and electrostatic term (▲, △) (*a*) in the native state, (*b*) in EXT, and (*c*) in NTV, respectively. *Solid line*, forward calculation; *dashed line*, reverse calculation.

components, $\Delta\Delta G_{LJ}$ and $\Delta\Delta G_{cov}$, dominantly contribute to $\Delta\Delta G^{NTV}$.

In Table 4, ΔG_{nonbd} is partitioned into protein-protein ($\Delta G_{pro\text{-}pro}$) and protein-water ($\Delta G_{pro\text{-}wat}$) components. Because the mutation site is fully buried in the hydrophobic core in the native state as shown in Fig. 1, $\Delta G_{pro\text{-}wat}$ was much smaller than $\Delta G_{pro\text{-}pro}$ in the native state. In EXT, the mutation site is more exposed to solvents than in NTV. Therefore, the magnitude of $\Delta G_{pro\text{-}wat}$ in EXT was greater than that in NTV. The contribution of $\Delta\Delta G_{pro\text{-}wat}$ to $\Delta\Delta G_{nonbd}$ is about the same as that of $\Delta\Delta G_{pro\text{-}pro}$ in NTV.

Free energy component analysis in detail: decomposition into residues

Nonbonded free energy differences are divided into the residual components to determine which residues contribute significantly to the change in stability. As shown in Fig. 4, the residues far from the mutation site along the sequence, as well as neighboring residues of the mutation site, contribute significantly to the total nonbonded free energy component. In Fig. 1, the protein residues whose $|\Delta\Delta G_{residue\ \alpha}|$ are greater than 0.03 kcal/mol are shown by ball-and-stick models in the native-state structure. The residues that contribute significantly to $\Delta\Delta G^{EXT}$ are located either in the same hydrophobic core (F3, L8, Y38, N39, T40, and I89) in the native state in which the mutation site exists, or at the neighboring region of the mutation site along the sequence (D53, Y54, G55, F57). Except for D53 and Y54, all of the residues are in contact with the mutation site. As shown in Fig. 5, the contributions from D53 and Y54 to ΔG_D^{EXT} were relatively large, whereas those to ΔG_D^{NTV} were quite small.

All of the residues that contribute significantly to $\Delta\Delta G^{NTV}$ are located in the hydrophobic core (F3, L8, Y38, N39, T40, and I89) in the native state. They are very close to the mutation site. In the native state, all of the atoms in these residues were always located within 9 Å of the C^{δ} atom of I56 during the calculations. As shown in Fig. 5, the free energy components of the neighboring region (D53, Y54, G55, F57) in the native state are quite similar to those in the denatured state. Although the residual components of G55 and F57 to ΔG_N were significant, they cancel the ΔG_D components of the corresponding residues (in Fig. 5). This cancellation does not take place in the case of $\Delta\Delta G^{EXT}$, $\Delta\Delta G^{RND1}$, $\Delta\Delta G^{RND2}$, and $\Delta\Delta G^{RND3}$. This is why $\Delta\Delta G^{EXT}$, $\Delta\Delta G^{RND1}$, $\Delta\Delta G^{RND2}$, and $\Delta\Delta G^{RND3}$ are significantly larger than $\Delta\Delta G^{exp}$.

Free energy component analysis in detail: decomposition into chemical groups

Judging from the results, it is strongly suggested that the native-like structure is appropriate for the residual structure near the mutation site. To obtain a physical picture of this mutation in detail, $\Delta\Delta G^{NTV}$ are decomposed into chemical groups that are included in the residues of the hydrophobic core (F3, L8, Y38, N39, T40, and I89). In Table 5, chemical groups in these residues, whose magnitude of the nonbonded free energy components is larger than 0.01 kcal/mol, are listed. Side-chain chemical groups (methyl and methylene groups) in the hydrophobic residues (F3, L8, and I89), as well as main-chain chemical groups (amide and carbonyl groups) in the hydrophilic residues (Y38, N39, and T40) contribute significantly to $\Delta\Delta G^{NTV}$.

DISCUSSIONS

Evaluation of the models for the denatured state

In this section, we evaluate the models of the denatured state in terms of the results obtained in the present study. As discussed in the Introduction, the approximation involved in the peptide model consisting of five residues is that only the neighboring residues of the mutation site contribute significantly to free energy changes in the denatured state, i.e., $\Delta G_{pept\text{-}rest} = 0$. In fact, we have shown in the previous paper (Sugita and Kitao, 1998) that free energy components of ΔG_{nonbd} vanish rapidly as interatomic distances increase. It is known experimentally that protein structures in the de-

TABLE 3 Free energy components, covalent (cov), Lennard-Jones (LJ), and electrostatic (el)

	Denatured state model	Total (kcal/mol)*	cov (kcal/mol)*	LJ (kcal/mol)*	el (kcal/mol)*
ΔG_N	—	−0.02 ± 0.21	0.85 ± 0.07	−1.54 ± 0.10	0.67 ± 0.04
ΔG_D	EXT	−2.40 ± 0.06	0.39 ± 0.01	−3.00 ± 0.04	0.21 ± 0.01
	NTV	−1.01 ± 0.12	0.47 ± 0.05	−2.14 ± 0.08	0.66 ± 0.02
$\Delta\Delta G$	EXT	2.38 ± 0.22	0.46 ± 0.07	1.46 ± 0.10	0.46 ± 0.04
	NTV	0.99 ± 0.24	0.38 ± 0.09	0.60 ± 0.13	0.01 ± 0.05

*The meaning of ± is the same as in Table 2.

natured states are less compact than those in the native states. Therefore, $\Delta G_{\text{pept-rest}}$ is expected to be negligible if "rest" residues are distant enough from the mutation site in the denatured state.

In the present study, we have employed five-residue peptides in the denatured state simulations. In the native state, we note that, except for F57, free energy contributions of the neighboring residues along the sequence are negligibly small. Therefore, in the native-like model, the use of five residues is sufficient for the model of the denatured state. In the case of the extended peptide, the contribution from the terminal residue (53) is not negligible, as shown in Fig. 5*b*. To examine the dependence of ΔG_D on the segment size of the peptides, we have carried out an additional ΔG_D calculation by starting from the seven-residue peptide of extended structure. $\Delta\Delta G^{cal}$ obtained in the calculation was 2.40 ± 0.27 kcal/mol. The difference between seven- and five-residue peptide models is within the range of error and is negligible. Therefore, we think that the use of five residues is sufficient for both the extended and native-like models of the denatured state.

Because free energy calculation is well established as giving a reasonable free energy value when structure is determined in atomic detail, we think ΔG_N is reliable. If $\Delta G_{\text{pept-rest}}$ is negligible in the denatured state, the structure in the vicinity of the mutation site dominantly determines ΔG_D. As can be seen in Table 2, $\Delta\Delta G^{cal}$ was in good agreement with $\Delta\Delta G^{exp}$ only when NTV was employed for the denatured state. In the other cases, $\Delta\Delta G^{cal}$ were largely overestimated. It is strongly suggested that the structure in the vicinity of the mutation site in the denatured state is native-like.

In NTV, mild constraints were added to the backbone atoms to retain native-like structure. To examine their effect on $\Delta\Delta G^{cal}$, we have carried out two additional ΔG_D calculations by starting from the same native-like structure with different strengths of the constraints. In the first case, no constraints were applied. In this case, the native-like structure changed largely during reverse calculation (V to I). Therefore, the hysteresis errors were significantly large. However, $\Delta\Delta G^{cal}$ obtained in the forward calculation (V to I) was in good agreement with $\Delta\Delta G^{exp}$. This indicates that $\Delta\Delta G^{cal}$ close to $\Delta\Delta G^{NTV}$ for the mild constraints is obtained without constraints if the structure is determined to be native-like. In the second case, the strength of the constraints was five times stronger than the mild one. $\Delta\Delta G^{cal}$ obtained with this calculation was 0.88 ± 0.22 kcal/mol, which is quite close to $\Delta\Delta G^{NTV}$ for the mild constraints, 0.99 ± 0.24 kcal/mol. Thus $\Delta\Delta G^{cal}$ obtained by using native-like initial structure does not depend significantly on the magnitude of constraints. In the model with the strong constraints, the RMSDs of (ϕ, ψ) angles of the mutated residue, 6.8, 5.9 (in degrees), are less than those in the native state, 8.1, 7.6, and in the mild constraints, 11.0, 11.4. Because the structure in the denature state is expected to be more flexible than that in the native state, the mild constraints used in NTV appear to be appropriate.

Side-chain rotamer states in NTV were the same as those in the native state, except for the terminal residue (Q58). The difference in the rotamer states in Q58 involves the χ_3 angle. The difference may be caused by the lack of hydrophobic interactions with some of the "rest" residues that are in contact with Q58 in the native state.

Comparison with other models of the denatured state

In the recent studies of Dobson and co-workers (Fiebig et al., 1996; Smith et al., 1996a, b; Schwalbe et al., 1997), local protein structure in the denatured state has been theoretically modeled by using a random coil polypeptide model, which is based on amino-acid-specific (ϕ, ψ) distributions extracted from the Protein Data Bank. The modeled

TABLE 4 Nonbonded, protein-protein, and protein-water free energy components

	Denatured state model	Nonbonded (kcal/mol)*	Protein-protein (kcal/mol)*	Protein-water (kcal/mol)*
ΔG_N	—	−0.87 ± 0.14	−0.94 ± 0.08	0.07 ± 0.07
ΔG_D	EXT	−2.79 ± 0.05	−2.39 ± 0.11	−0.40 ± 0.06
	NTV	−1.48 ± 0.06	−1.27 ± 0.01	−0.20 ± 0.08
$\Delta\Delta G$	EXT	1.89 ± 0.15	1.45 ± 0.14	0.47 ± 0.09
	NTV	0.60 ± 0.16	0.33 ± 0.08	0.28 ± 0.10

*The meaning of ± is the same as in Table 2.

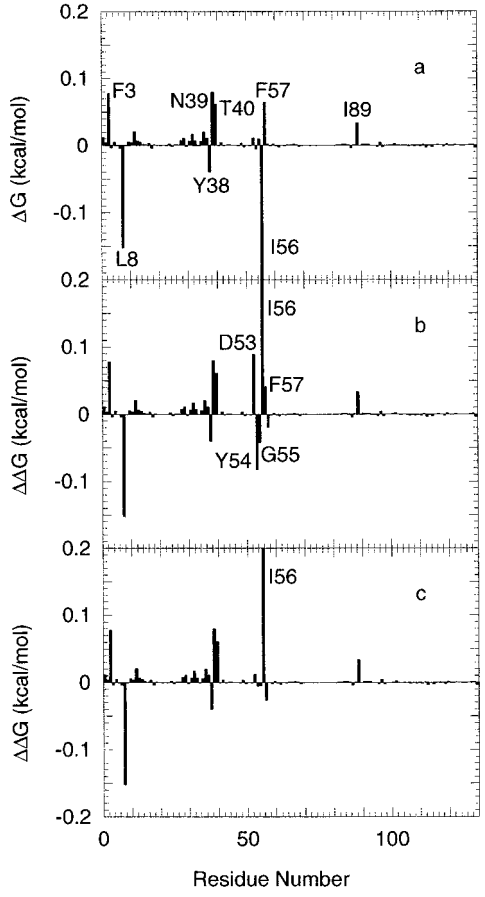

FIGURE 4 Residual nonbonded components of (*a*) ΔG_N, (*b*) $\Delta\Delta G^{EXT}$, and (*c*) $\Delta\Delta G^{NTV}$. These components of I56 are out of the range of the figure. They are (*a*) −1.18, (*b*) 1.51, and (*c*) 0.31 kcal/mol.

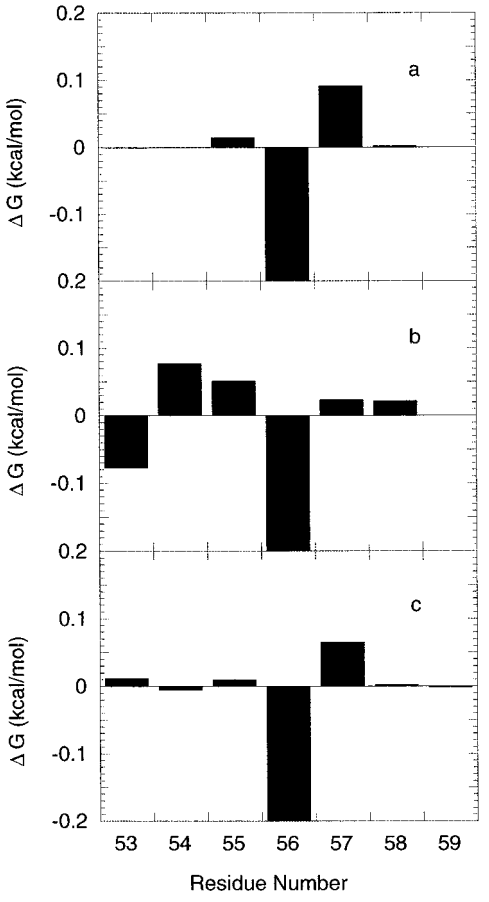

FIGURE 5 Nonbonded contributions from the neighboring residues of the mutation site, (*a*) to ΔG_N, (*b*) to ΔG_D^{EXT}, and (*c*) to ΔG_D^{NTV}, respectively. These components of I56 are out of the range of the figure. They are (*a*) −1.18, (*b*) −2.69, and (*c*) −1.48 kcal/mol.

structure has been compared with the results of NMR measurements. Dobson et al. have applied their method to hen lysozyme denatured in 8 M urea at low pH. They have found four regions that deviate significantly from this random coil model. The mutation site in the present study is not included in the four regions, which implies that the structure of our mutation site is not native-like (Schwalbe et al., 1997). This disagreement may be due to the difference in the denaturation conditions, i.e., thermal denaturation in the present study and 8 M urea denaturation in their studies. Although our method is different from theirs, both works strongly pointed out the importance of studying structures in the denatured states. To understand the physical nature of protein stability, it is essential to investigate structures in the denatured states both experimentally and theoretically.

Analysis in terms of both native and denatured state structures

From experimental studies of protein stability, several empirical rules have been proposed to explain the Gibbs free energy changes at the different locations of the mutation sites (Eriksson et al., 1992; Pace, 1992; Serrano et al., 1992). For example, a statistical correlation has been found between $\Delta\Delta G$ and the number of methylene and methyl groups within a sphere of 6-Å radius surrounding the deleted methylene group in barnase (Serrano et al., 1992). In T4 lysozyme, $\Delta\Delta G$ have been explained in terms of the hydrophobicity of the side chain and the size of the cavity created by substitutions (Eriksson et al., 1992). However, the above correlation has not necessarily been observed for mutations in other proteins, such as human lysozyme (Takano et al., 1995). Because these rules are based on the implicit assumption that ΔG_D does not contribute to $\Delta\Delta G$ dominantly, it is natural that they do not have general applicability. As we have shown in the present study, $\Delta\Delta G$ strongly depends on the structure of the denatured state. By considering these results, we propose the following strategy to investigate the effects of mutations on protein stability.

Computational strategy to investigate effects of mutations on protein stability

1) Collect structural information on both the native and denatured states. 2) Carry out free energy simulation in the

TABLE 5 Chemical groups whose nonbonded free energy components are significantly large

Residue	Site	Group	LJ (kcal/mol)*	el (kcal/mol)*	Nonbonded (kcal/mol)*
F3	Cβ	—CH_2—	0.010 ± 0.001	0.004 ± 0.000	0.013 ± 0.001
	Cε	═CH—	0.011 ± 0.002	0.000 ± 0.000	0.011 ± 0.002
	Cδ	═CH—	0.022 ± 0.010	0.004 ± 0.001	0.026 ± 0.010
L8	Cγ	>CH—	0.022 ± 0.003	0.001 ± 0.000	0.023 ± 0.003
	Cδ	—CH_3	−0.052 ± 0.071	0.000 ± 0.000	−0.052 ± 0.071
	Cδ	—CH_3	−0.140 ± 0.006	0.000 ± 0.000	−0.140 ± 0.006
Y38	N	—NH—	0.017 ± 0.000	−0.003 ± 0.000	0.014 ± 0.001
	Cα	>CH—	−0.054 ± 0.026	0.002 ± 0.000	−0.051 ± 0.026
	Cβ	—CH_2—	0.022 ± 0.001	0.000 ± 0.000	0.021 ± 0.001
	Cδ	═CH—	0.018 ± 0.000	0.000 ± 0.000	0.017 ± 0.000
	C	>C═O	−0.062 ± 0.081	0.003 ± 0.002	−0.059 ± 0.008
N39	N	—NH—	0.023 ± 0.001	−0.004 ± 0.000	0.019 ± 0.001
	C	>C═O	0.039 ± 0.003	0.007 ± 0.001	0.046 ± 0.004
T40	N	—NH—	0.020 ± 0.000	0.000 ± 0.000	0.020 ± 0.000
	C	>C═O	0.009 ± 0.001	0.002 ± 0.000	0.011 ± 0.001
I89	Cγ	—CH_3	0.011 ± 0.004	0.000 ± 0.000	0.011 ± 0.000
	Cδ	—CH_3	0.010 ± 0.003	0.000 ± 0.000	0.010 ± 0.003

*The meaning of ± is the same as in Table 2.

native state to determine ΔG_N. 3) Carry out the residual component analysis of ΔG_N and decide how many residues should be included in the denatured state simulation if the native-like peptide model is to be employed. 4) Carry out the calculation of ΔG_D by using various models considering possible protein structures of the denatured state. 5) Compare the results of free energy calculations with experimental values and judge which model for the denatured state is appropriate. 6) Describe the effect of the mutation based on the structures in both the native and denatured states. Considering free energy components, specify the type of interaction (Lennard-Jones, electrostatic, etc.) and which residues dominantly contribute to $\Delta\Delta G$.

CONCLUSION

The effect of the I56V mutation on the thermal stability of human lysozyme was studied by free energy calculations. To calculate small free energy difference with high accuracy, a program package with very accurate treatments of the nonbonded energy calculations was employed. To study the dependence of the calculated free energy difference on the model structures of the denatured state, five different structures, extended, native-like, and three random-coil-like structures, were examined as the initial structures of the peptide. The calculated free energy difference, $\Delta\Delta G^{cal}$, is significantly dependent on the structure. When the native-like structure model is used, $\Delta\Delta G^{cal}$ is in good agreement with the free energy difference determined experimentally. It is strongly suggested that the structure in the vicinity of the mutation site takes native-like rather than extended or random-coil conformations.

To understand the physical nature of the I56V mutation, $\Delta\Delta G^{cal}$ determined by using the native-like model is examined by free energy component analysis. It has been shown that free energy components originating from Lennard-Jones and covalent interactions dominantly determine $\Delta\Delta G^{cal}$. The contribution of protein-protein interactions to $\Delta\Delta G_{nonbd}$ is about the same as that from protein-water interactions. From the residual free energy components, it is shown that the protein residues that are located in the hydrophobic core (F3, L8, Y38, N39, T40, and I89), in which the mutation site exists, contribute significantly to the nonbonded free energy component. From the further component analysis of these residues, it is shown that side-chain chemical groups (methyl and methylene groups) in the hydrophobic residues (F3, L8, and I89), as well as main-chain chemical groups (amide and carbonyl groups) in the hydrophilic residues (Y38, N39, and T40) contribute significantly to $\Delta\Delta G^{cal}$.

In this paper, we proposed a strategy to investigate the effects of mutations on protein stability. Details of the models for the denatured state (e.g., the number of residues constituting a peptide model, the structure of the peptide model) should be considered carefully, depending on proteins, mutation sites, etc. To show the usefulness of this strategy, applications to other mutations will be reported elsewhere (Sugita et al., 1998).

We are grateful to Prof. Nobuhiro Go for essential support of the research and research environment. We thank Prof. Katsuhide Yutani for providing us the x-ray coordinates and the thermodynamic data of the wild-type and mutant human lysozyme. We also express our thanks to Prof. Benoît Roux for providing us FORTRAN subroutines for the SSBP calculation. Computations were made at the Computer Centers of Kyoto University, Center for Promotion of Computational Science and Engineering of JAERI, Computer Centers of the Institute for Molecular Science, and by CRAY J916 in our laboratory.

This work was supported by grants from the Ministry of Education, Science and Culture, Japan (to AK).

REFERENCES

Beglov, D., and B. Roux. 1994. Finite representation of an infinite bulk system: solvent boundary potential for computer simulations. *J. Chem. Phys.* 100:9050–9063.

Beveridge, B. L., and F. M. DiCapua. 1989. Free energy via molecular simulation: application to chemical and biomolecular systems. *Annu. Rev. Biophys. Biophys. Chem.* 18:431–492.

Boresch, S., G. Archontis, and M. Karplus. 1994. Free energy simulations: the meaning of the individual contributions from a component analysis. *Proteins Struct. Funct. Genet.* 20:25–33.

Boresch, S., and M. Karplus. 1995. The meaning of component analysis: decomposition of the free energy in terms of specific interaction. *J. Mol. Biol.* 254:801–807.

Brady, G. P., and K. A. Sharp. 1995. Decomposition of interaction free energies in proteins and other complex systems. *J. Mol. Biol.* 254:77–85.

Brady, G. P., A. Szabo, and K. A. Sharp. 1996. On the decomposition of free energies. *J. Mol. Biol.* 263:123–125.

Buck, M., S. E. Radford, and C. M. Dobson. 1994. Amide hydrogen exchange in a highly denatured state: hen egg-white lysozyme in urea. *J. Mol. Biol.* 237:247–254.

Dill, K. A., and D. Shortle. 1991. Denatured states of proteins. *Annu. Rev. Biochem.* 60:795–825.

Ding, H.-Q., N. Karasawa, and W. A. Goddard, III. 1992. Atomic level simulations on million particles: the cell multipole method for Coulomb and London nonbond interactions. *J. Chem. Phys.* 97:4309–4315.

Eriksson, A. E., W. A. Baase, X.-J. Zhang, D. W. Heinz, M. Blaber, E. P. Baldwin, and B. W. Matthews. 1992. Response of a protein structure to cavity-creating mutations and its relation to the hydrophobic effect. *Science.* 255:178–183.

Evans, P. A., K. D. Topping, D. N. Woolfson, and C. M. Dobson. 1991. Hydrophobic clustering in nonnative states of a protein: interpretation of chemical shifts in NMR spectra of denatured states of lysozyme. *Proteins Struct. Funct. Genet.* 9:248–266.

Fersht, A. R., and L. Serrano. 1993. Principles of protein stability derived from protein engineering experiments. *Curr. Opin. Struct. Biol.* 3:75–83.

Fiebig, K. M., H. Schwalbe, M. Buck, L. J. Smith, and C. M. Dobson. 1996. Toward a description of the conformations of denatured states of proteins. Comparison of a random coil model with NMR measurements. *J. Phys. Chem.* 100:2661–2666.

Flanagan, J. M., M. Kataoka, T. Fujisawa, and D. M. Engelman. 1993. Mutations can cause large changes in the conformation of a denatured protein. *Biochemistry.* 32:10359–10370.

Funahashi, J., K. Takano, K. Ogasahara, Y. Yamagata, and K. Yutani. 1996. The structure, stability, and folding process of amyloidogenic mutant human lysozyme. *J. Biochem.* 120:1216–1223.

Hoover, W. G. 1985. Canonical dynamics: equilibrium phase-space distributions. *Phys. Rev. A.* 31:1695–1697.

Jorgensen, W. L., J. Chandrasekhar, and J. D. Madura. 1983. Comparison of simple potential functions for simulating liquid water. *J. Chem. Phys.* 79:926–935.

Jorgensen, W. L., and C. Ravimohan. 1985. Monte Carlo simulation of differences in free energies of hydration. *J. Chem. Phys.* 83:3050–3054.

Kataoka, M., and Y. Goto. 1996. X-ray solution scattering studies of protein folding. *Folding Des.* 1:107–114.

Kellis, J. J. T., K. Nyberg, and A. R. Fersht. 1989. Energetics of complementary side-chain packing in a protein hydrophobic core. *Biochemistry.* 28:4914–4922.

Kollman, P. 1993. Free energy calculations: applications to chemical and biochemical phenomena. *Chem. Rev.* 93:2395–2417.

Kraulis, P. J. 1991. MOLSCRIPT: a program to produce both detailed and schematic plots of protein structures. *J. Appl. Crystallogr.* 24:946–950.

Lattman, E. E. 1994. Small angle scattering studies of protein folding. *Curr. Opin. Struct. Biol.* 4:87–92.

Mathews, B. W. 1993. Structural and genetic analysis of protein stability. *Annu. Rev. Biochem.* 62:139–160.

Merrit, E. A., and M. E. P. Murphy. 1994. Raster3D Version 20. A program for photorealistic molecular graphics. *Acta Crystallogr. D.* 50:869–873.

Morikami, K., T. Nakai, A. Kidera, M. Saito, and H. Nakamura. 1992. PRESTO (PRotein Engineering SimulaTOr): a vectorized molecular mechanics program for biopolymers. *Comput. Chem.* 16:243–248.

Nosé, S. 1984. A molecular dynamics method for simulations in the canonical ensemble. *Mol. Phys.* 52:255–268.

Otzen, D. E., and A. R. Fersht. 1995. Side-chain determinants of beta-sheet stability. *Biochemistry.* 34:5718–5724.

Otzen, D. E., M. Rheinnecker, and A. R. Fersht. 1995. Structural factors contributing to the hydrophobic effect: the partly exposed hydrophobic minicore in chymotrypsin inhibitor 2. *Biochemistry.* 34:13051–13058.

Pace, C. N. 1992. Contribution of the hydrophobic effect to globular protein stability. *J. Mol. Biol.* 226:29–35.

Radford, S. E., M. Buck, K. D. Topping, C. M. Dobson, and P. A. Evans. 1992. Hydrogen exchange in native and denatured states of hen egg-white lysozyme. *Proteins Struct. Funct. Genet.* 14:237–248.

Saito, M., and R. Taninura. 1995. Relative melting temperatures of RNase HI mutant proteins from MD simulation/free energy calculations. *Chem. Phys. Lett.* 236:156–161.

Schwalbe, H., K. M. Fiebig, M. Buck, J. A. Jones, S. B. Grimshaw, A. Spencer, S. J. Glaser, L. J. Smith, and C. M. Dobson. 1997. Structural and dynamical properties of a denatured protein. Heteronuclear 3D NMR experiments and theoretical simulations of lysozyme in 8 M urea. *Biochemistry.* 36:8977–8991.

Serrano, L., J. T. Kellis, Jr., P. Cann, A. Matouschek, and A. R. Fersht. 1992. The folding of an enzyme. II. Substructure of barnase and the contribution of different interactions to protein stability. *J. Mol. Biol.* 224:783–804.

Shortle, D. 1996. The denatured state (the other half of the folding equation) and its role in protein stability. *FASEB J.* 10:27–34.

Shortle, D., W. E. Stites, and A. K. Meeker. 1990. Contributions of the large hydrophobic amino acids to the stability of staphylococcal nuclease. *Biochemistry.* 29:8033–8041.

Smith, L. J., K. A. Bolin, H. Schwalbe, M. W. MacArthur, J. M. Thornton, and C. M. Dobson. 1996a. Analysis of main chain torsion angles in proteins: prediction of NMR coupling constants for native and random coil conformations. *J. Mol. Biol.* 255:494–506.

Smith, L. J., K. M. Fiebig, H. Schwalbe, and C. M. Dobson. 1996b. The concept of a random coil. Residual structure in peptides and denatured proteins. *Folding Des.* 1:95–106.

Smith, P. E., and W. F. van Gunsteren. 1994. When are free energy components meaningful? *J. Phys. Chem.* 98:2366–2379.

Straatsma, T. P., and J. A. McCammon. 1992. Computational alchemy. *Annu. Rev. Phys. Chem.* 43:407–435.

Sugita, Y., and A. Kitao. 1998. Improved protein free energy calculation by more accurate treatment of nonbonded energy: application to chymotrypsin inhibitor 2, V57A. *Proteins Struct. Funct. Genet.* 30:388–400.

Sugita, Y., A. Kitao, and N. Go. 1998. Computational analysis of thermal stability: effect of Ile to Val mutations in human lysozyme. *Folding Des.* 3:173–181.

Sun, Y.-C., D. L. Veenstra, and P. A. Kollman. 1996. Free energy calculations of the mutation of Ile^{96} to Ala in barnase: contribution of the difference in stability. *Protein Eng.* 9:273–281.

Takano, K., K. Ogasahara, H. Kaneda, Y. Yamagata, S. Fujii, E. Kanaya, M. Kikuchi, M. Oobatake, and K. Yutani. 1995. Contribution of hydrophobic residues to the stability of human lysozyme: calorimetric studies and x-ray structural analysis of the five isoleucine to valine mutants. *J. Mol. Biol.* 254:62–76.

Takano, K., Y. Yamagata, S. Fujii, and K. Yutani. 1997. Contribution of the hydrophobic effect to the stability of human lysozyme: calorimetric studies and x-ray structural analyses of the nine valine to alanine mutants. *Biochemistry.* 36:688–698.

Tanimura, R., and M. Saito. 1996. Molecular dynamics/free energy perturbation studies of the thermostable V74I mutant of ribonuclease HI. *Mol. Simulation.* 16:75–85.

Tidor, B., and M. Karplus. 1991. Simulation analysis of the stability mutant R96H of T4 lysozyme. *Biochemistry.* 30:3217–3228.

van Gunsteren, W. F., and A. E. Mark. 1992. On the interpretation of biochemical data by molecular dynamics computer simulation. *Eur. J. Biochem.* 204:947–961.

Weiner, S. J., P. A. Kollman, D. T. Nguyen, and D. A. Case. 1986. An all atom force field for simulations of proteins and nucleic acids. *J. Comput. Chem.* 7:230–252.

Yun-yu, S., A. Mark, E. W. Cun-xin, H. Fuhua, H. J. C. Berendsen, and W. F. van Gunsteren. 1993. Can the stability of protein mutants be predicted by free energy calculations? *Protein Eng.* 6:289–295.